

# Internal Oxidation and Nitridation of Hot Rolled Steels - A Theoretical Study and its Experimental Verification



Max-Planck-Institut  
für Eisenforschung GmbH

Gunnar Eriksson Symposium &  
GTT-Technologies Annual Workshop and Users' Meeting  
Herzogenrath-Kohlscheid (Aachen, Germany)



Christian Doppler  
Forschungsgesellschaft

12<sup>th</sup> July, 2012

**voestalpine**

EINEN SCHRITT VORAUS.



## **Max-Planck-Institut für Eisenforschung GmbH**

Head: Prof. Dierk Raabe



Founded in 1917 from the “Kaiser Wilhelm Institute”  
by Fritz Wüst.

### 3 Departments:

Computational Materials Design

Interface Chemistry and Surface Engineering

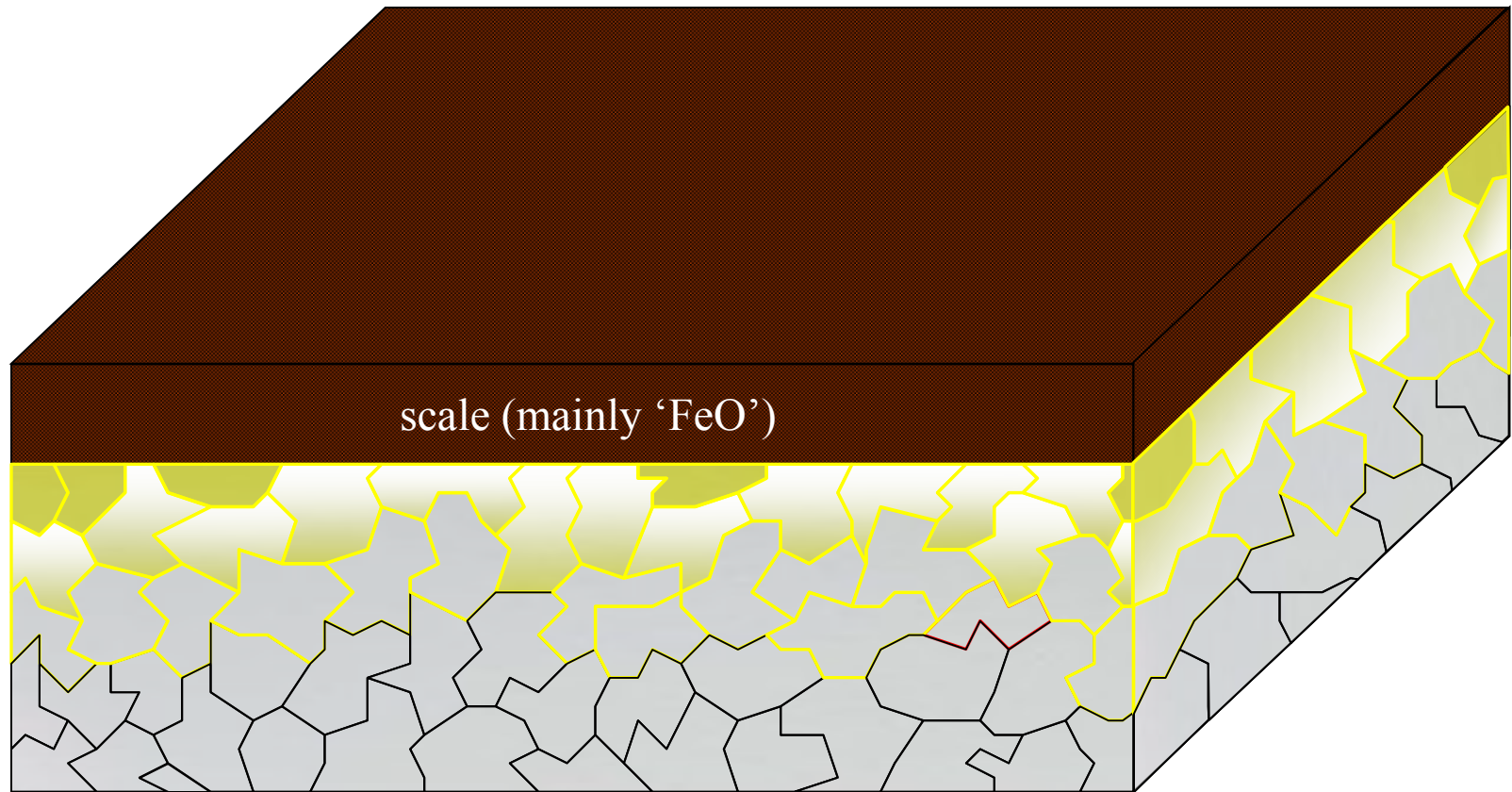
Microstructure Physics and Alloy Design

- Motivation
- Theoretical Calculations
  - Programme Algorithm and Possibilities
  - Oxygen and Nitrogen Diffusion
- Some Examples
  - HT-Corrosion in binary and ternary Alloys
  - Important Modelling Effects
- Conclusion

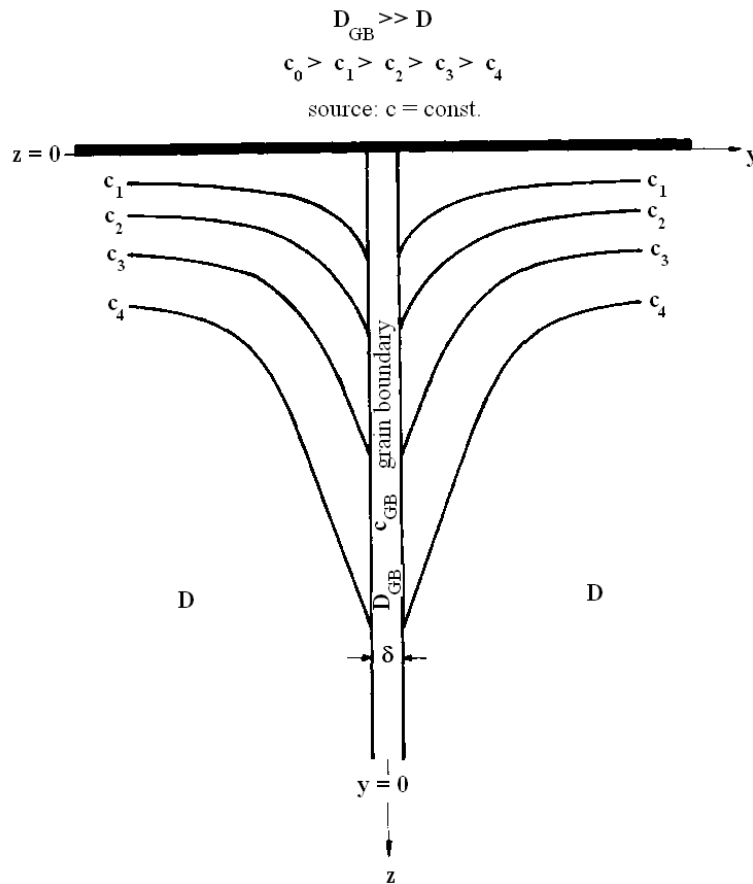






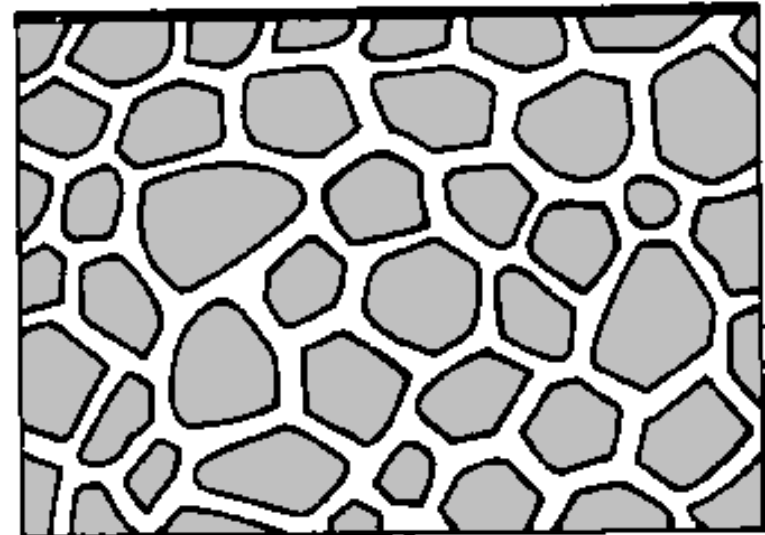


# Fisher's Model of Diffusion



*Whipple – Le Claire equation*

$$s \delta D_{GB} = 0.3292 \sqrt{\frac{D}{t}} \left( \frac{\partial \log \bar{c}}{\partial z^{6/5}} \right)^{-\frac{5}{3}}$$



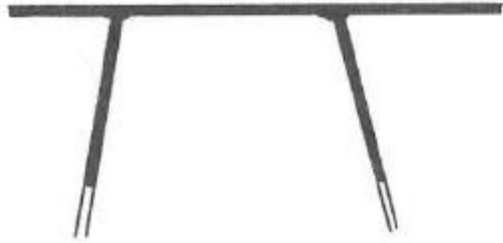
*Levine – MacCallum equation*

$$s \delta D_{GB} = 0.4704 \sqrt{\frac{D}{t}} \left( \frac{\partial \log \bar{c}}{\partial z^{6/5}} \right)^{-\frac{5}{3}}$$

# Grain Boundary Diffusion Regimes



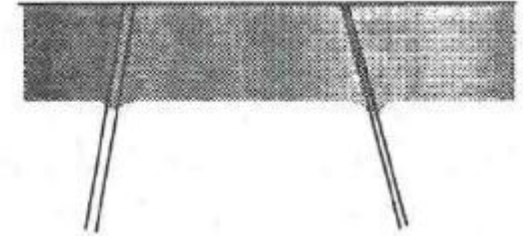
Coarse grained



C – regime

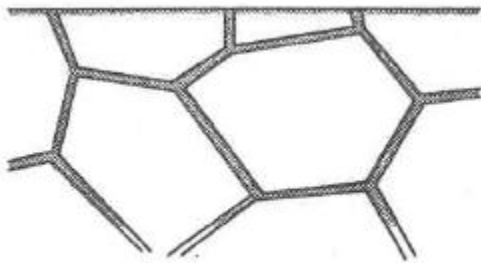


B – regime

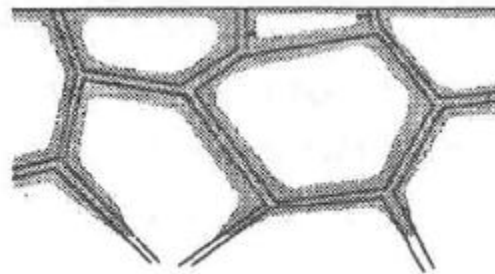


A – regime

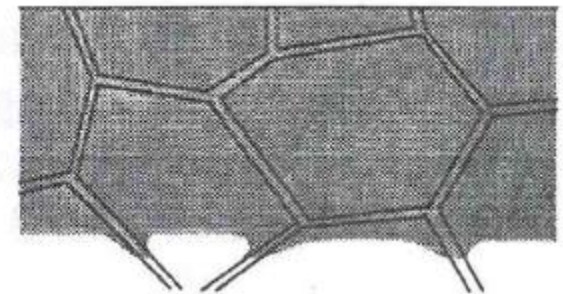
Fine grained



C' – regime



B' – regime



A' – regime

**Figure:** Illustration of different diffusion regimes, depending on total diffusion time and ratio of  $D_{GB}/D$ .



Pergamon



ELSEVIER

Inst  
M

com

Temperature  
in Ar-H<sub>2</sub>-H<sub>2</sub>

D.J. Young<sup>a</sup>, J. Z

Depart<sup>a</sup> School of Materials Science  
<sup>b</sup> Forschungszentrum Jülich

## ARTICLE IN

### Abstract

A coup  
phase tem  
as well as  
multiple c  
a γ-Ni-27

constitution of the developing  
oxidation stage, whereas the  
parabolic oxide-layer growth r  
© 2003 Acta Materialia Inc. P

Keywords: Modelling; Thermodyn

### Article history:

Received 1 December 2011  
Accepted 22 February 2011  
Available online 26 Febru

### Keywords:

A. Steel  
B. TEM  
C. Oxidation

## 1. Introduction

Internal corrosion is a generic kind of material degradation occurring at high temperatures that is driven by the inward diffusion of a corrosive species (i.e., oxygen, nitrogen, carbon, or sulfur, followed by internal precipitation of the respective oxides, nitrides, carbides, and sulfides).<sup>[1]</sup> Contrary to the formation of superficial scales, which in the case of Cr<sub>2</sub>O<sub>3</sub> and Al<sub>2</sub>O<sub>3</sub> protect the substrate against excessive corrosion attack,<sup>[2]</sup> internal corrosion may result in a deep deterioration of the physical properties of the material (e.g., creep resistance and high-temperature fatigue strength).<sup>[3,4]</sup> Figure 1 shows an example of internal oxidation (Al<sub>2</sub>O<sub>3</sub>) and nitridation (AlN; penetration depth ξ = 600 μm) underneath a thin Cr<sub>2</sub>O<sub>3</sub> scale.

The mechanism of internal corrosion depends on the local concentrations and the diffusivities of the corrosive species and the metallic elements in the substrate. For the example shown in Fig. 1, a low oxygen partial pressure,  $p(\text{O}_2)$ , relative to the nitrogen partial pressure  $p(\text{N}_2)$  in the combustion gas leads to conditions in the material interior, for

## Internal Corrosion of Engineering Alloys: Experiment and Computer Simulation

Ulrich Krupp and Hans J. Christ

(Submitted July 18, 2005)

High-temperature corrosion is generally known as a material degradation process that occurs at the surface of engineering components. In the case of internal corrosion, the corrosive species penetrates into the material by solid-state diffusion leading to the formation of internal precipitates, for instance, oxides (internal oxidation), nitrides (internal nitridation), and carbides (carburation). It is known from numerous publications and technical failure cases that internal corrosion results in a strong deterioration of the properties of a material (i.e., near-surface embrittlement or the dissolution of strengthening phases). The present article introduces the classic theory of internal oxidation and reviews some recent research on internal corrosion phenomena that are closely related to the failure mechanisms of thermally grown protective oxide scales on several commercial high-temperature alloys (e.g., single-crystalline and polycrystalline Ni-base alloys and Cr steels). The mechanisms and kinetics of internal corrosion processes are determined by the temperature, the local chemical composition of the material, the solubility and diffusivity of the corrosive species, as well as the mechanical loading conditions. These influence factors are taken into account by means of a computer model combining a numerical finite-difference approach to solve the diffusion differential equations with the thermodynamic tool ChemApp. Using several examples, it is shown that the model has been applied successfully to simulate the internal nitridation, carburation, and oxidation of high-temperature alloys.

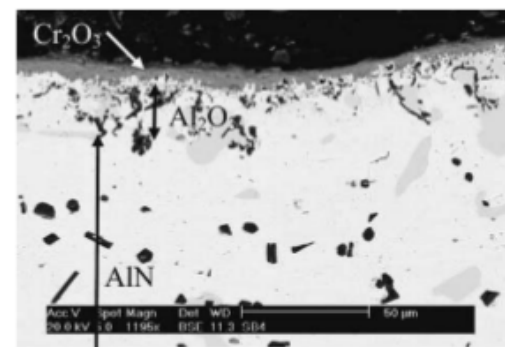


Fig. 1 Internal oxidation and nitridation attack of a failed natural gas burner tube of alloy 601 operated at  $T = 1100^\circ\text{C}$

which AlN instead of Al<sub>2</sub>O<sub>3</sub> is the thermodynamically most stable compound.\*

Even in the case of Al<sub>2</sub>O<sub>3</sub>-scale-forming Ni-base super-

ion

ence

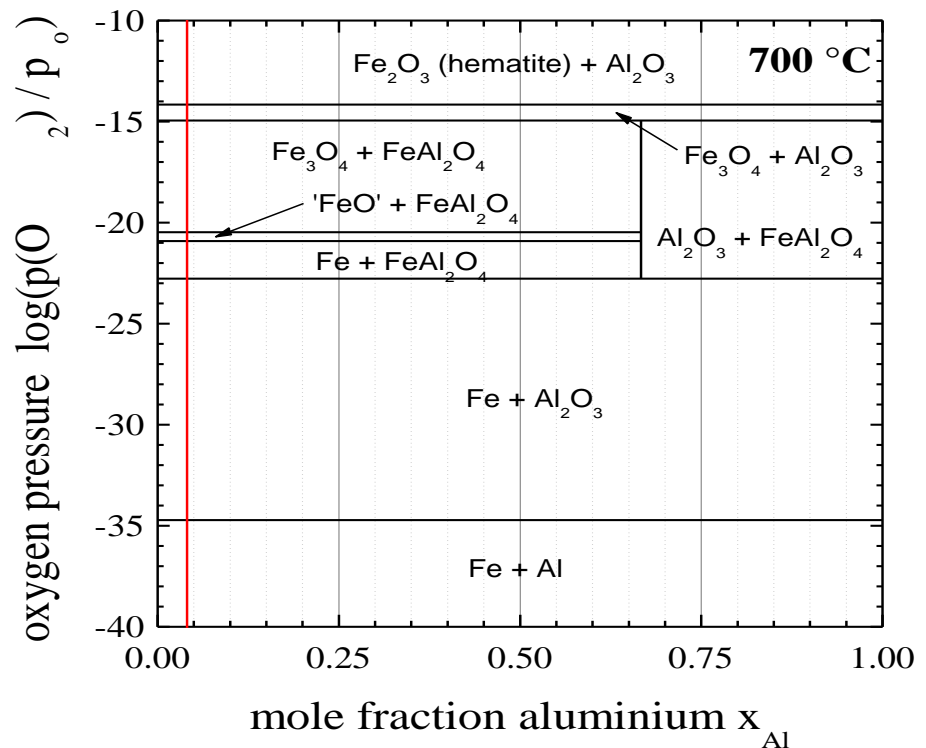
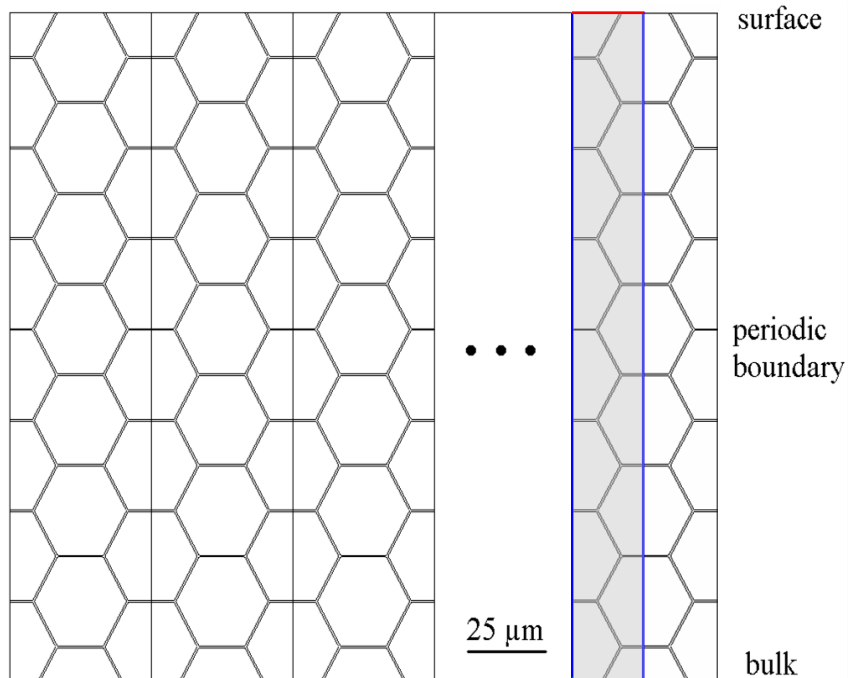
e



element migration

chemical reaction

$$\frac{dc_{i(x,t)}}{dt} = \text{div}(D_{i(x,T)} \cdot \nabla c_{i(x,t)})$$



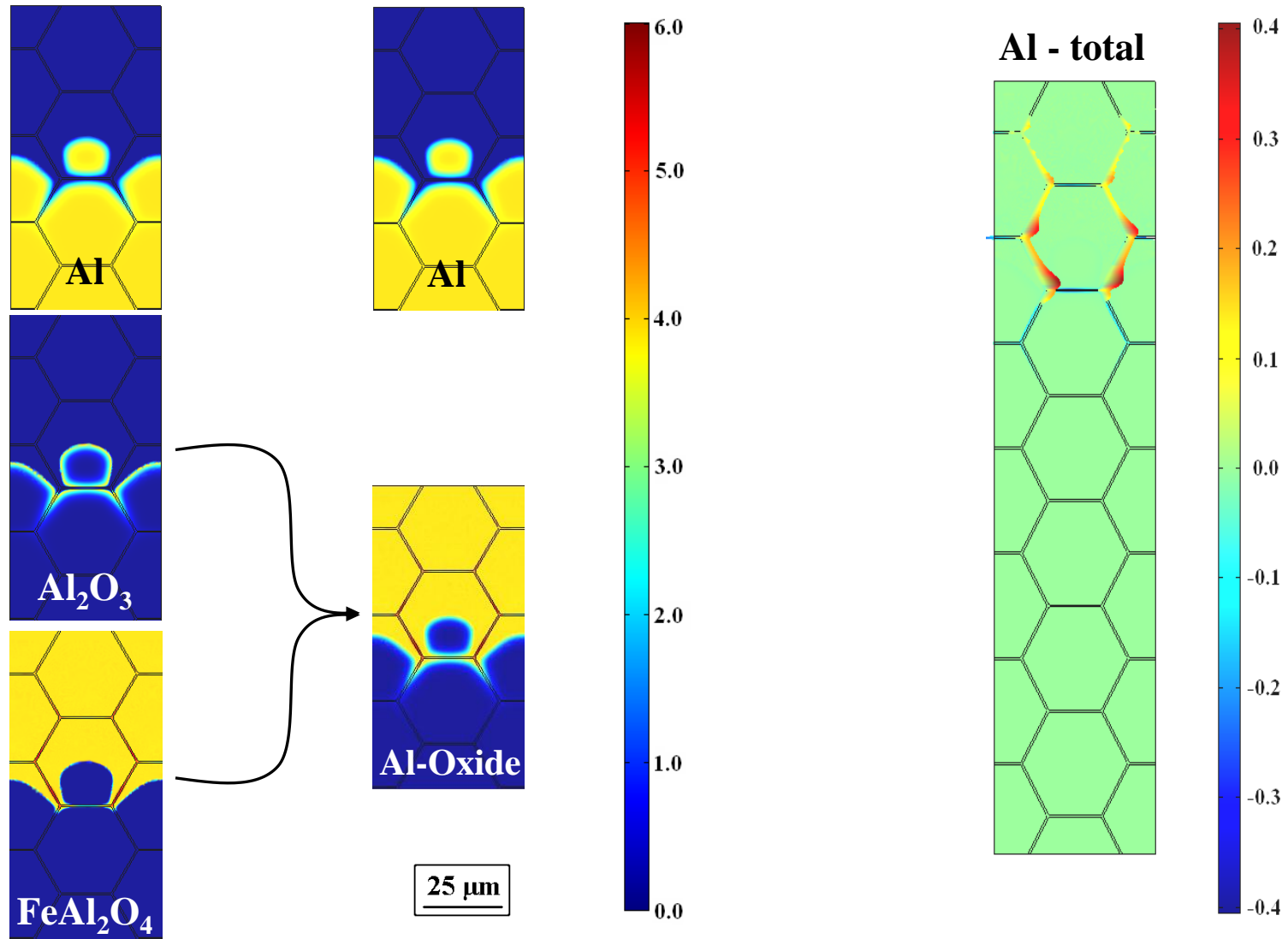


**Figure:** Spatial phase distributions of Fe, 2 wt-% Al (4.05 mol-% Al) after oxidation at  $p(\text{O}_2) = 10^{-22}$  bar for 60 min at 700 °C.

# Oxide Stability

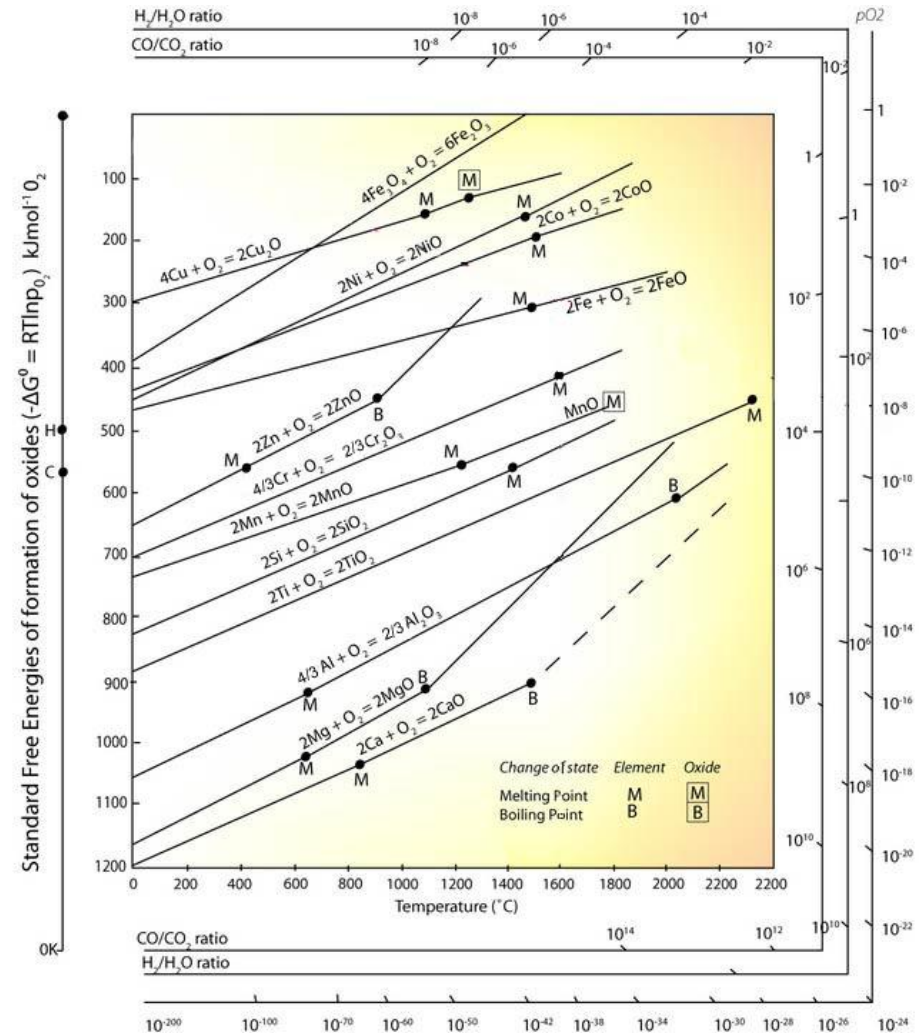
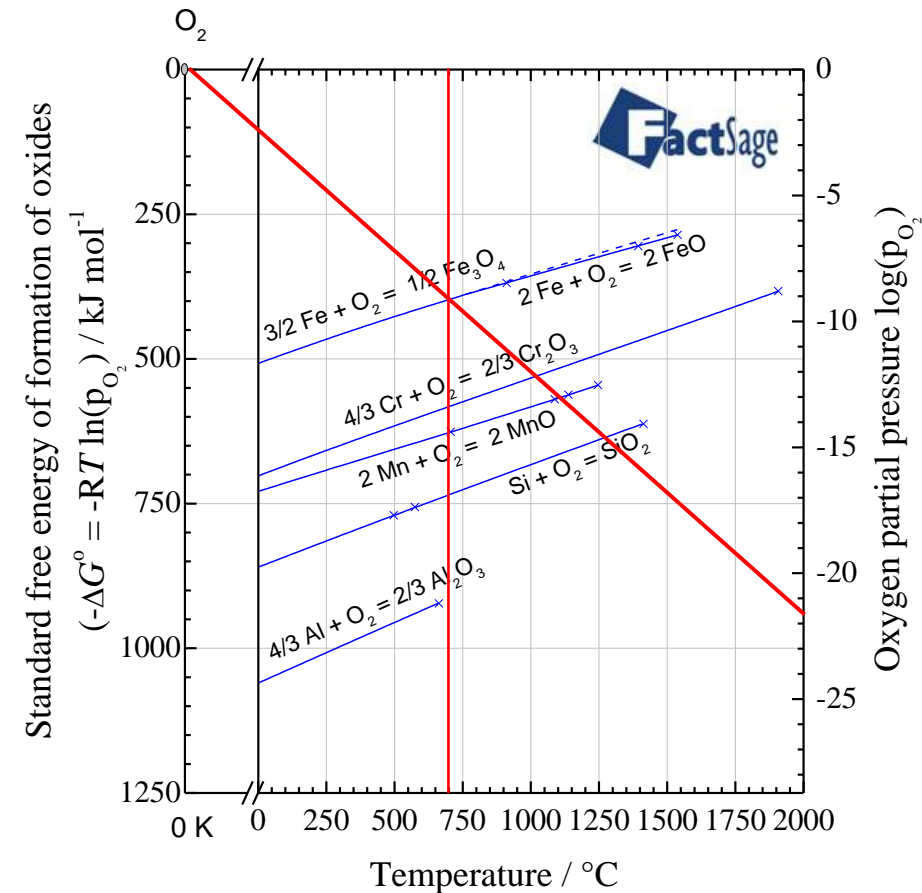


**Figure:** Calculated and experimentally determined Ellingham-Diagrams for the Oxide Stability of Iron, Chromium, Manganese, Silicon and Aluminium.

# Iron – Manganese – Chromium alloy

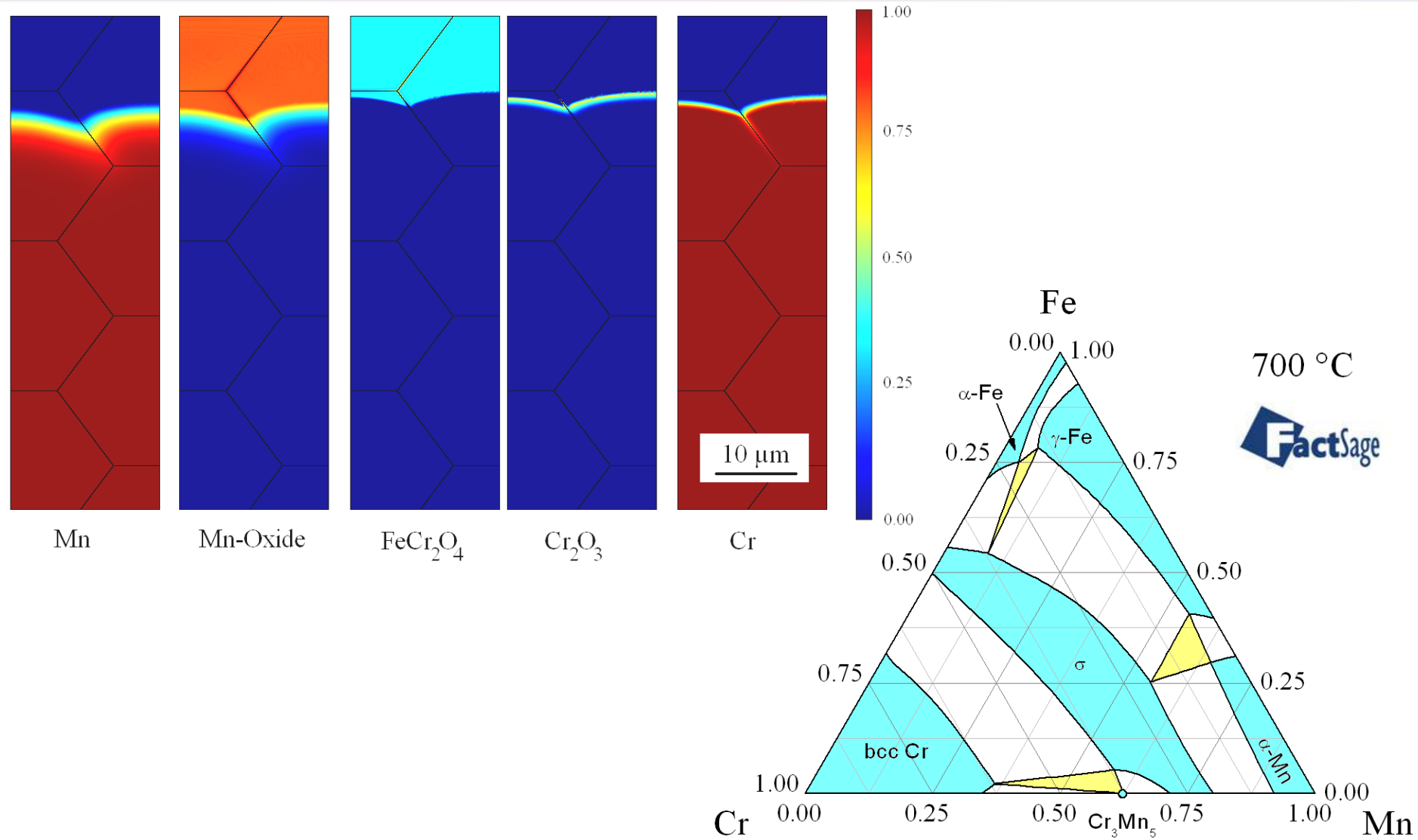


**Figure:** Spatial phase distribution in an Fe, 2 wt-% Mn, 0.8 wt-% Cr alloy after oxidation at  $p(\text{O}_2) = 3 \cdot 10^{-22}$  bar and 700 °C for 120 min and ternary phase diagram.



## Nitride Stability

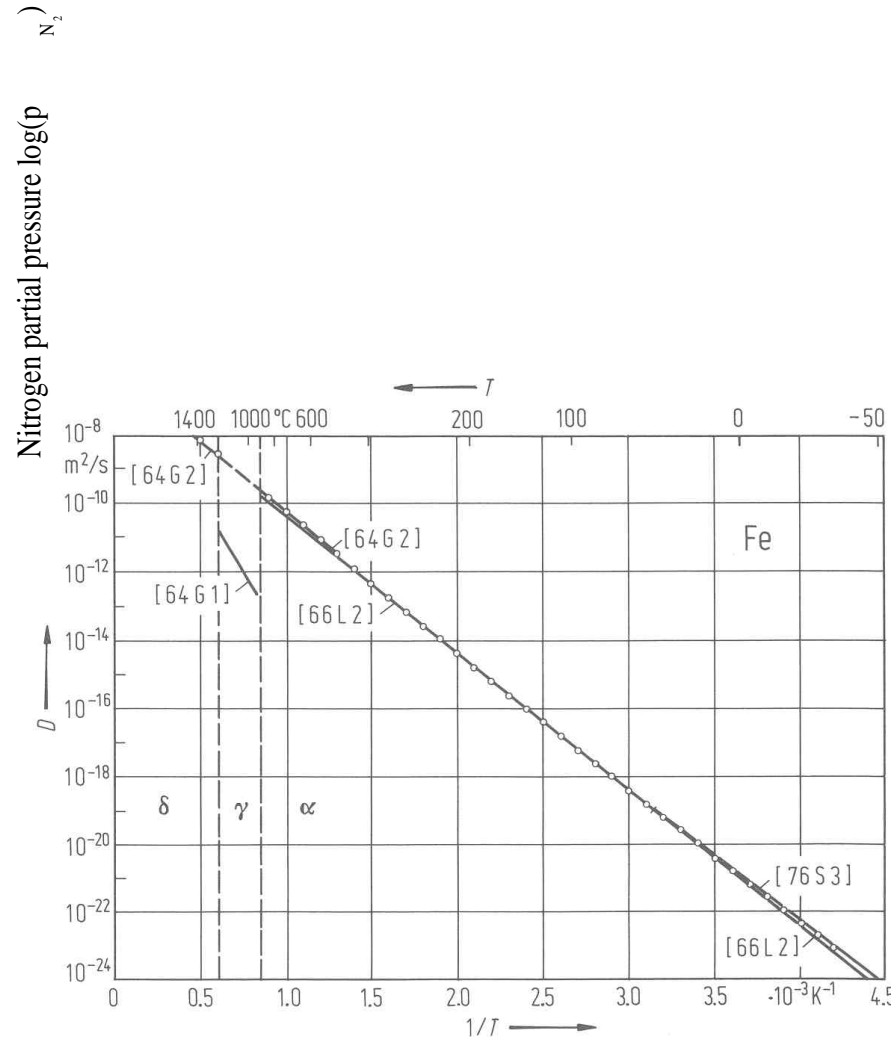
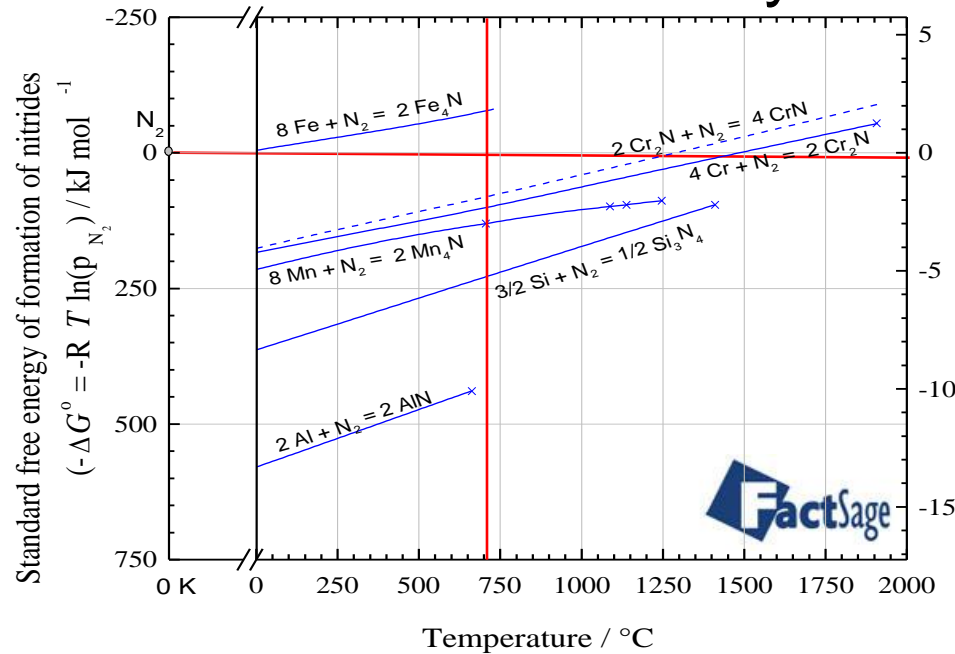
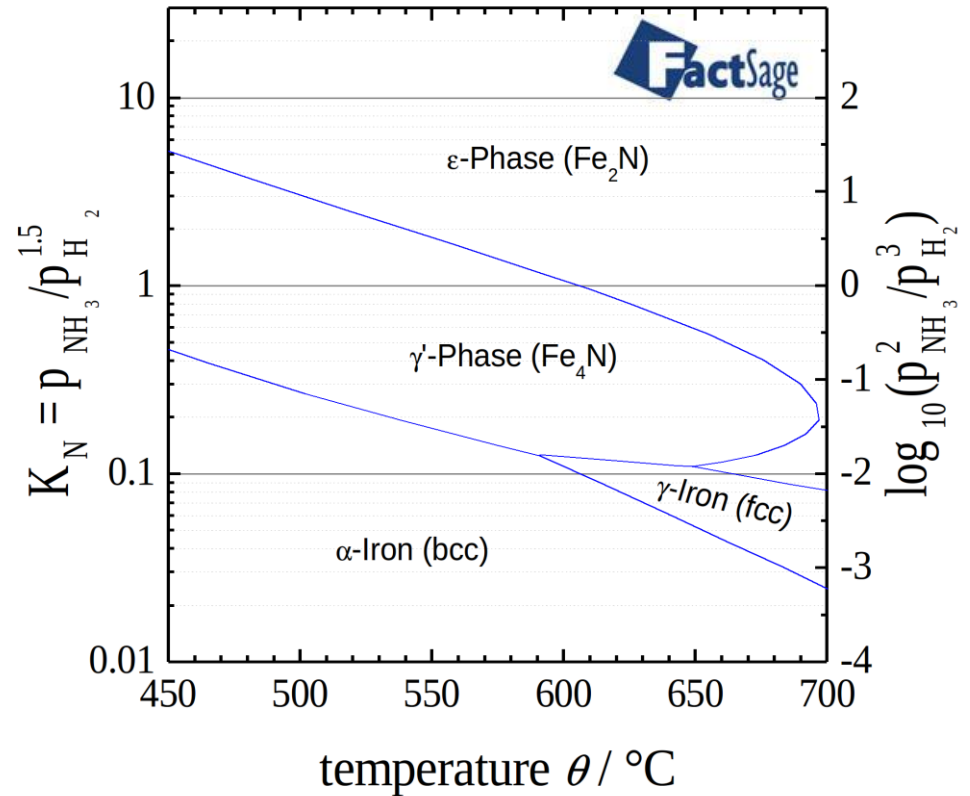
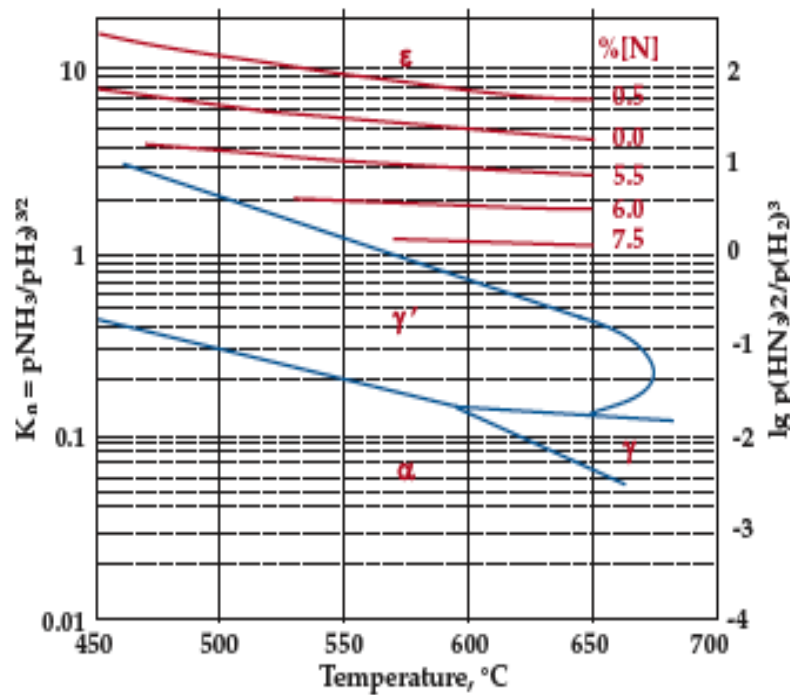
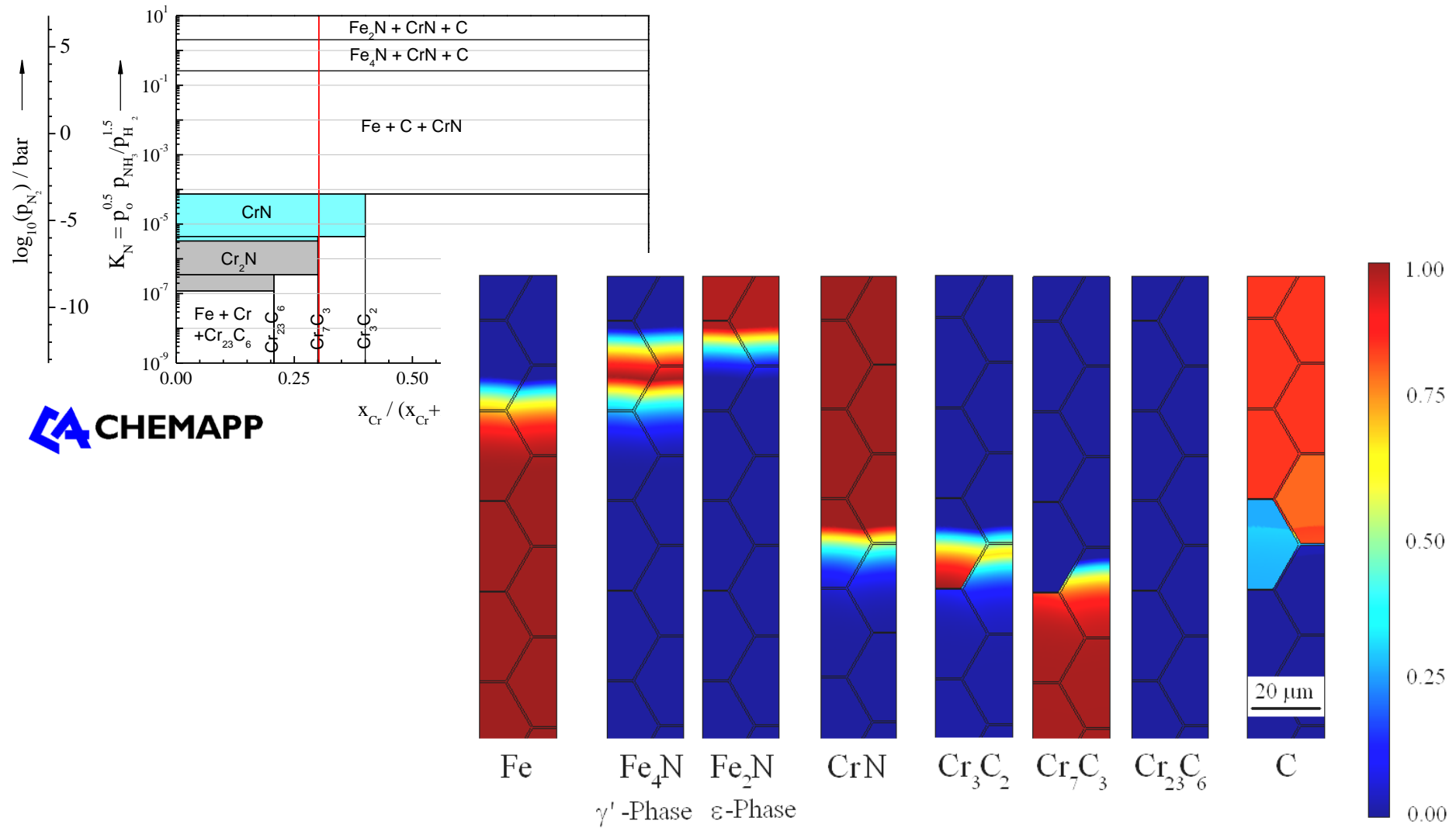


Fig. 22. Fe. Diffusion coefficient for N diffusion in  $\alpha$ ,  $\gamma$  and  $\delta$ -phase Fe vs. (reciprocal) temperature. Circles: calculated from equation quoted from [76S3].



**Figure:** Lehrer-Diagram of iron nitrides according to literature (left) and calculated with the programme FactSage (right).

# Iron – Chromium – Carbon alloy

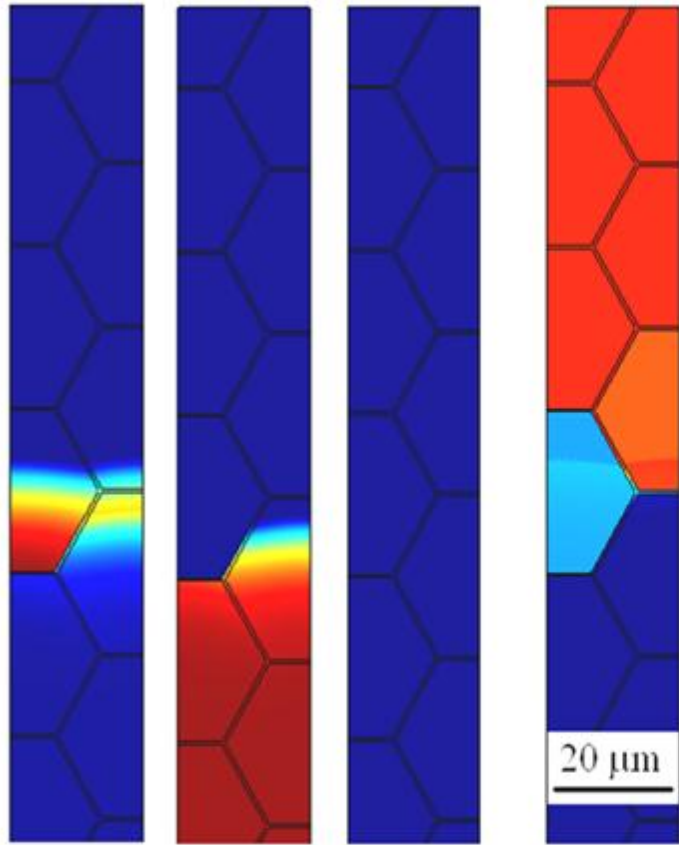


**Figure:** Spatial phase distribution in an Fe, 1 wt-% Cr, 0.1 wt-% C alloy after gas nitriding at  $K_N = 2.4$  and 500 °C for 48 h and phase stability diagram.

# Comparison of the SAE51xx steels

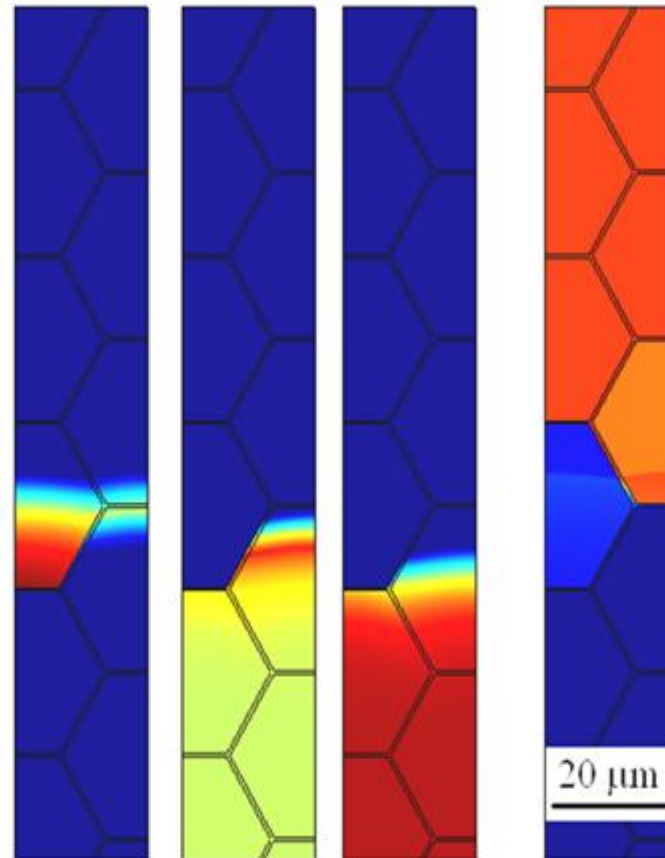


Fe, 1 wt-% Cr, 0.10 wt-% C



$\text{Cr}_3\text{C}_2$   $\text{Cr}_7\text{C}_3$   $\text{Cr}_{23}\text{C}_6$  C

Fe, 1 wt-% Cr, 0.08 wt-% C



$\text{Cr}_3\text{C}_2$   $\text{Cr}_7\text{C}_3$   $\text{Cr}_{23}\text{C}_6$  C

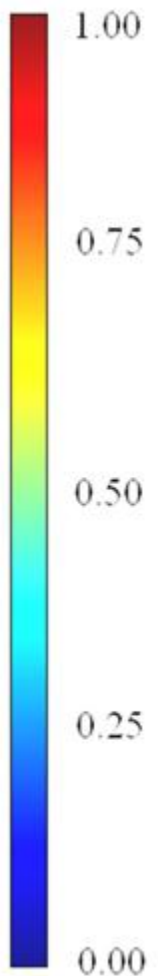


**Figure:** Comparison of the carbide phase distribution in two SAE51xx type steels after gaseous nitriding at  $K_N = 1\,000$  ( $p_{\text{tot}} = 1$  atm) and 500 °C for 48 h.



# „Real“ Steels

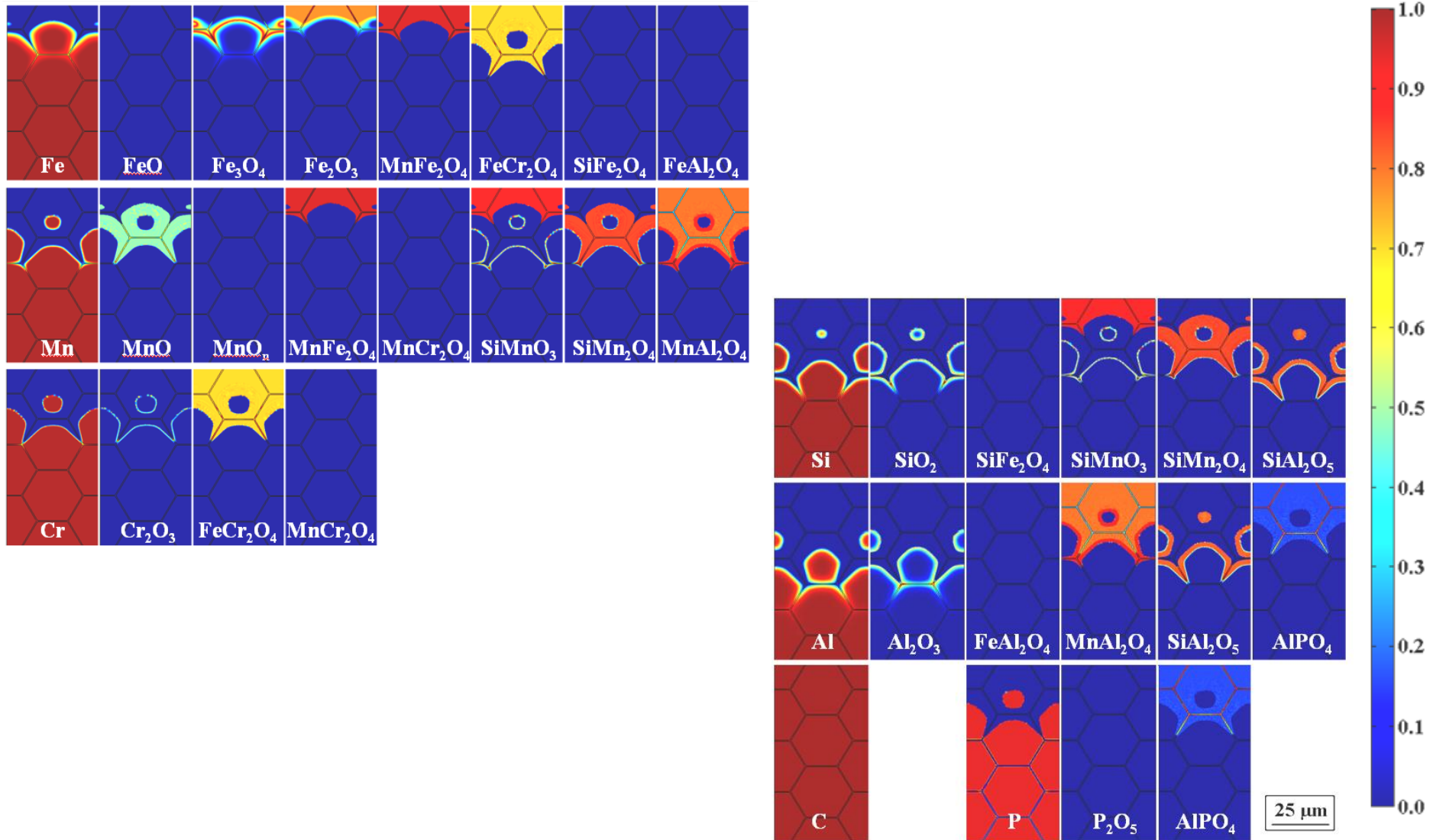


**Figure:** Calculated phase distribution of an industrial steel alloy after oxidation at  $p(\text{O}_2) = 10^{-22}$  bar and a technical cooling programme.

# Diffusion between different Phases



$$J_A = -D \nabla c$$

$$J_A = -L \nabla \mu$$

$$J_A = -L \nabla \mu = -L \frac{\partial \mu}{\partial c} \nabla c = \dots = -L \underbrace{\frac{RT}{c}}_D \nabla c - L \left( \nabla \mu^o + \frac{RT}{\gamma} \nabla \gamma \right)$$

**Figures:** Shibuya (渋谷) crossing in Tokyo with green and red pedestrian lights.

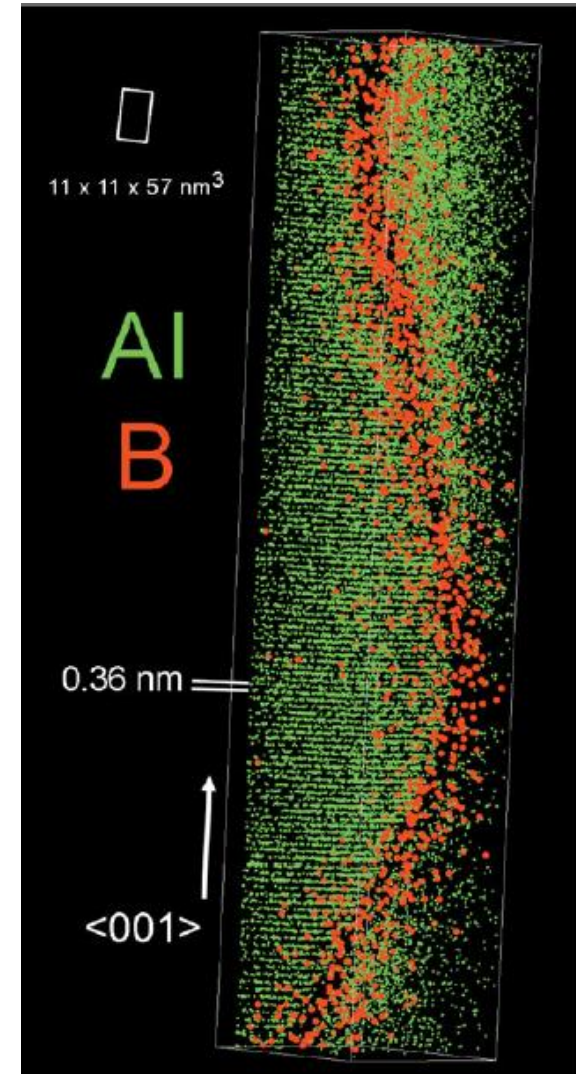
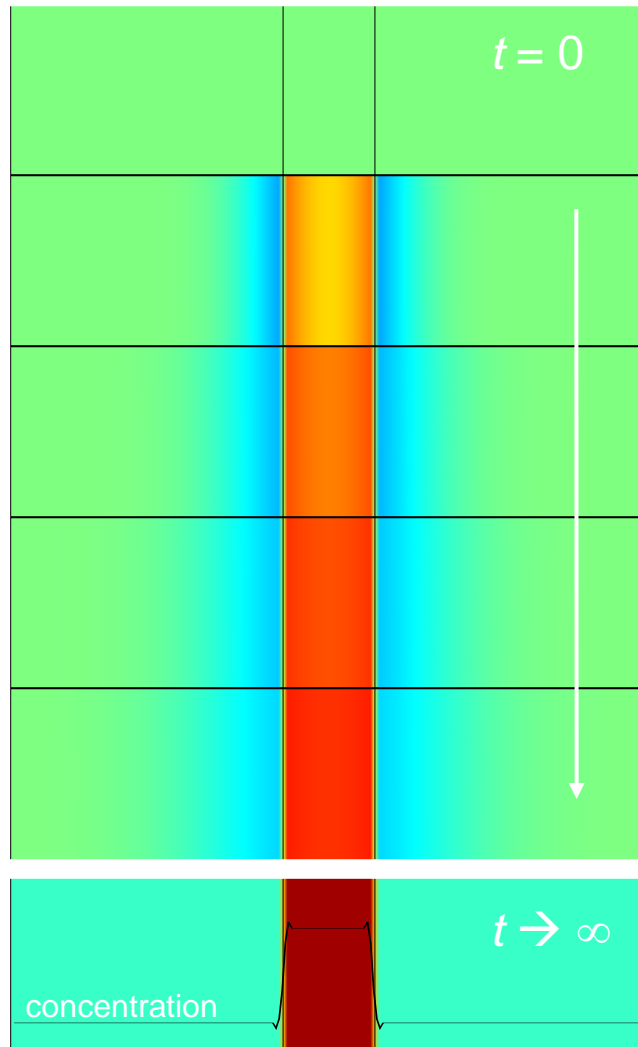


**Figure:** Numerical simulation of segregation (left) and 3D atom probe tomography of segregated boron atoms along the grain boundary in a NiAl superalloy [1] (right).



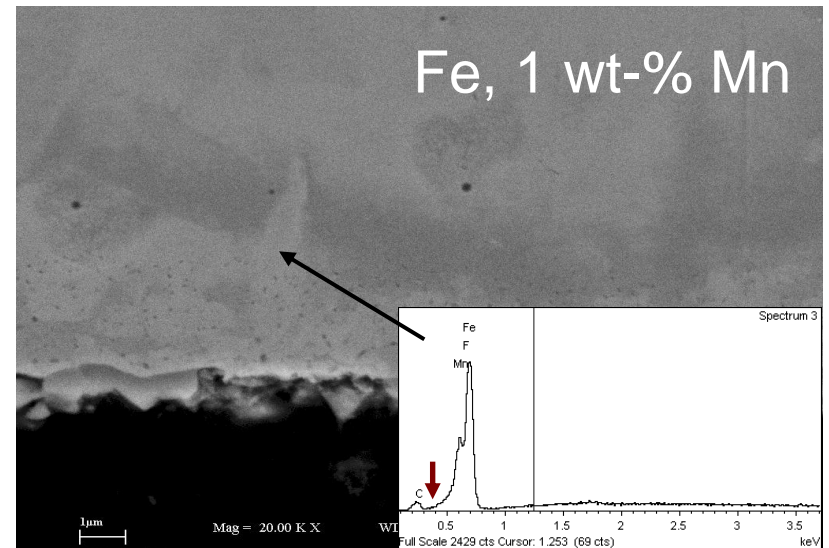
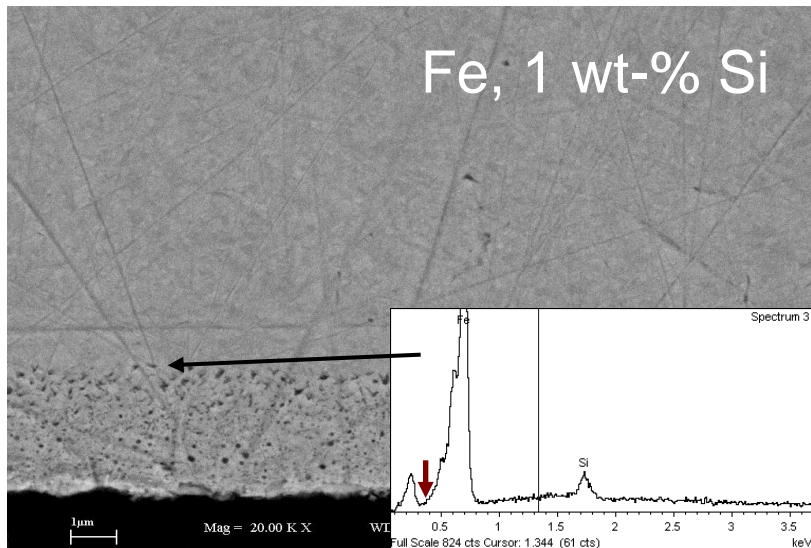
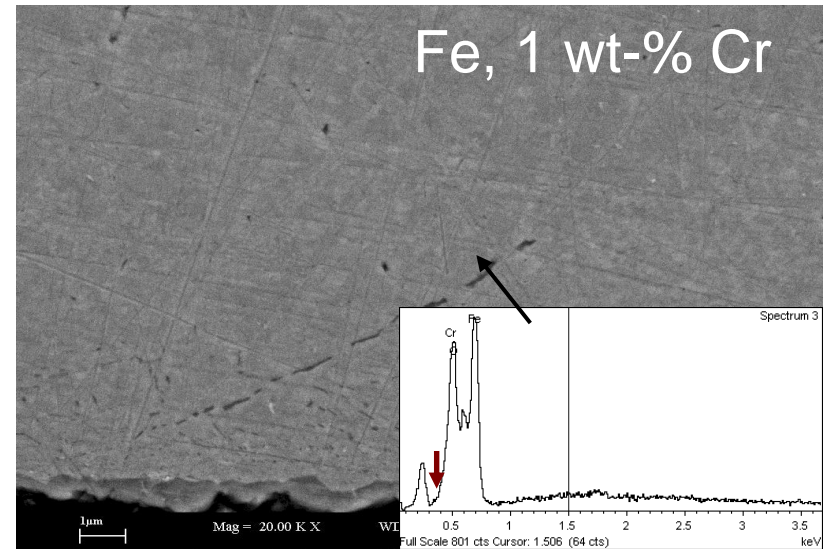
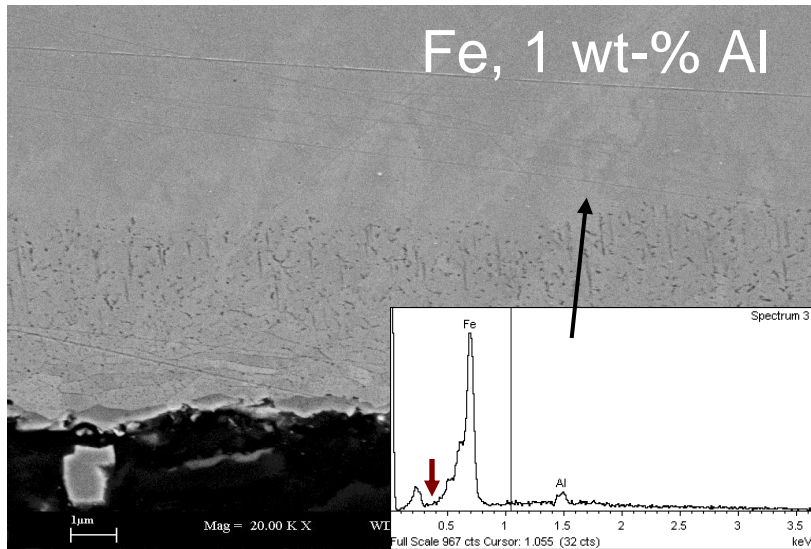


**Figure:** SEM and EDX-images of four different binary iron alloys, oxidised at 700 °C for 5 h in N<sub>2</sub> / 2.5 % H<sub>2</sub> / H<sub>2</sub>O (DP +8 °C). The red arrow marks the N signal position.



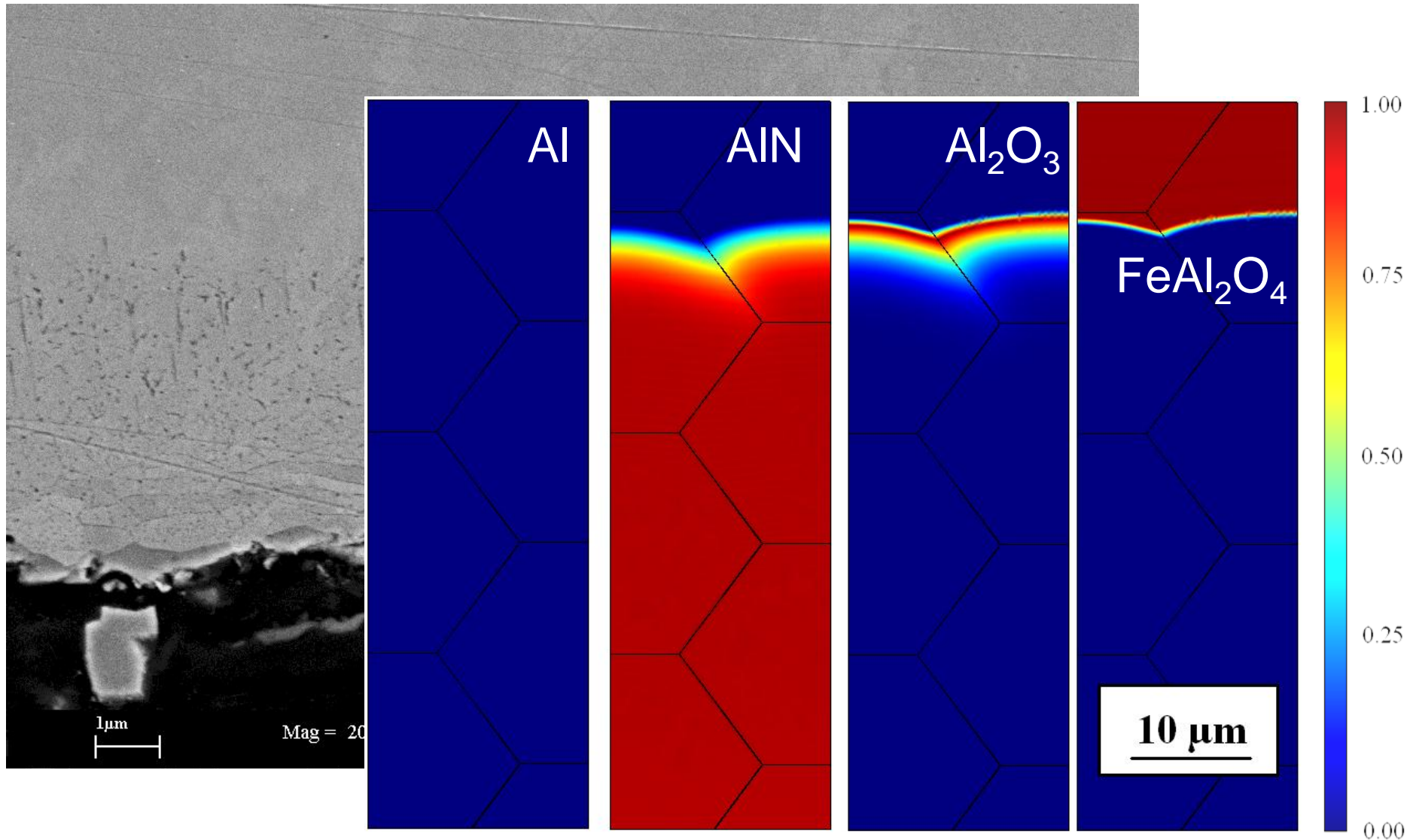


**Figure:** Fe, 1wt-%Al, oxidised at 700 °C for 5 h in N<sub>2</sub> / 2.5 vol-% H<sub>2</sub> / H<sub>2</sub>O (DP +8 °C). SEM-picture (left) and numerical simulation of the phase distribution (right).

- Reaction-Diffusion-Systems provide a powerful method to describe High Temperature Processes
- FactSage and ChemApp proved to be a valuable tool for making theoretical assumptions
- Good agreement with experimental values for oxidation depth and oxide formation
- Deviations between theory and experiment can be used to foster further research



Max-Planck-Institut  
für Eisenforschung GmbH

Dirk and Alexandra Vogel,  
Else-Marie Müller-Lorenz,  
Monika Nellessen



TECHNISCHE  
UNIVERSITÄT  
WIEN  
Vienna University of Technology

Prof. H. Danninger  
Vera G. Praig, Markus Holzweber,  
Kurt Piplits

**voestalpine**

EINEN SCHRITT VORAUS.

Dr. Paesold  
Bernhard Linder, Klaus Rendl

## Funding



Christian Doppler  
Forschungsgesellschaft

**voestalpine**

EINEN SCHRITT VORAUS.



